# Magnetoreflectance and magnetization of the semimagnetic semiconductor $Cd_{1-x}Fe_xSe$

A. Twardowski and K. Pakula
*Institute of Experimental Physics, Warsaw University, Hoza 69, 00681 Warsaw, Poland*

I. Perez, P. Wise, and J. E. Crow
*MARTECH, Florida State University, Tallahassee, Florida 32306-3016*
*and Department of Physics, Temple University, Philadelphia, Pennsylvania 19122*
(Received 15 May 1990)

Magnetoreflectance measurements of excitonic interband transitions are used to study exchange interaction between band electrons and localized Fe $d$ electrons in hexagonal $Cd_{1-x}Fe_xSe$ ($x \leq 0.13$) at $T=1.9$ K and $B \leq 5$ T. Combining exciton splitting with the magnetization of the same samples, we determined the difference between conduction- and valence-band exchange constants $N_0\alpha - N_0\beta = 1.85$ eV. Given from previous work $N_0\alpha = 0.25$ eV, the value $N_0\beta = -1.6$ eV is obtained. We also demonstrate that the band splittings are parametrized by macroscopic magnetization for the magnetic field oriented parallel as well as perpendicular to the crystal hexagonal axis. Additionally, we present a theoretical model for magnetization, $x < 0.05$.

## I. INTRODUCTION

Semimagnetic semiconductors (SMSC's) or diluted magnetic semiconductors are II-VI, II-V, IV-VI, or III-V compounds, where some nonmagnetic cations are substituted by magnetic ions of the transition-metal or rare-earth-metal elements.[1] These systems exhibit interesting magnetic and magneto-optical properties due to the exchange interaction between magnetic ions ($d$-$d$ exchange) as well as between magnetic ions and band electrons ($s,p$-$d$ exchange).[1] Most of the research performed so far has been devoted to SMSC's containing Mn as a magnetic ion, with the latter representing a rather simple case of a system of permanent magnetic moments associated with $Mn^{2+}$ ion spins ($S=\frac{5}{2}, L=0$). A more general situation is encountered for the class of Fe-based SMSC's,[2,3] because substitutional $Fe^{2+}$ ions have both spin and orbital momenta ($S=2, L=2$).[4,5] The energetical structure of the $Fe^{2+}$ dopant in II-VI compounds has been studied for a long time[4-8] and it was found[4,5] that the ground-state term $^5E$ is split into a singlet $A_1$ followed by a triplet $T_1$, a doublet $E$, a triplet $T_2$, and a singlet $A_2$. The separation between these levels is roughly 15 $cm^{-1}$. The next term $^5T$ is at about 3000 $cm^{-1}$ above the $^5E$ term.[9] Consequently, the situation for Fe is essentially different than for Mn: Fe ions reveal only a field-induced magnetic moment, leading to typical Van Vleck-type paramagnetism.[6,5] This magnetic behavior is also reflected in the magneto-optical properties of $Zn_{1-x}Fe_xSe$, $Cd_{1-x}Fe_xSe$, and $Hg_{1-x}Fe_xSe$.[10-14,1] The available data suggest that band splittings are parametrized by the macroscopic magnetization of an Fe ion system,[10,11,14] similarly as it was shown for Mn-type SMSC's.[1] Actually such a parametrization was really demonstrated only for $Zn_{1-x}Fe_xSe$ so far,[10] where band splittings were found to be a linear function of the macroscopic magnetization. In that respect interband spectroscopy provides a useful method of the determination of $s,p$-$d$ exchange constants in these materials.

Interband transitions in $Cd_{1-x}Fe_xSe$ have been studied recently by us.[14] However, no direct relation between band splittings and macroscopic magnetization could have been established, since magnetization data of the studied crystals were not available. Consequently $Cd_{1-x}Fe_xSe$ exchange constants were only estimated with the help of low-field susceptibility.[14]

In this paper we report complete magnetoreflectance measurements of excitonic interband transitions in a new set of $Cd_{1-x}Fe_xSe$ crystals, together with magnetization measurements performed on the same samples. Based on this data we obtained the exchange constants for conduction and valence bands.

In Sec. II we note the theoretical background necessary for interpreting the optical spectra of hexagonal SMSC's crystals. Experimental details of this work are given in Sec. III. The results are presented and discussed in Sec. IV (magnetization) and Sec. V (magnetoreflectance). We conclude in Sec. VI.

## II. THEORETICAL BACKGROUND

The $s,p$-$d$ exchange interaction between delocalized band electrons and Mn ions in Mn-based SMSC's was suggested (in the spirit of the mean-field theory and virtual crystal approximation) in the following form:[1,15]

$$H_{ex} = -JN_0x\langle \mathbf{S} \rangle \mathbf{s} , \quad (1)$$

where $\langle \mathbf{S} \rangle = (\langle S_x \rangle, \langle S_y \rangle, \langle S_z \rangle)$ is the mean value of the magnetic ion spins, $\mathbf{s}$ is the band electron spin, $J$ is the exchange constant, and $N_0$ is the number of unit cells in the unit volume.

The band splittings in Fe-based SMSC's resulting from the $s$-$d$ exchange interaction can, in general, be treated in a similar way, however, the exchange Hamiltonian (1) has

 

to be revised. This Hamiltonian is the correct one when the interacting states are simple multiplets,[16] as for materials containing $Mn^{2+}$. Although for the $Fe^{2+}$ case the situation is more complicated (all five multiplets resulting from the $^5E$ term should be considered, as well as the influence of the higher-lying $^5T$ term), we assume for further analysis an exchange Hamiltonian in the form (1) having in mind similar exciton behavior in Mn- and Fe-based SMSC's.[10]

The mean ion spin $\langle S \rangle$ in the $Mn^{2+}$ case was easily expressed by macroscopic magnetization (per unit mass):

$$M_m = (x/m)P \ , \tag{2}$$

where $P = -\mu_B \langle L + gS \rangle$ is the magnetic moment of an ion and $m = (1-x)x_{Zn} + xm_{Mn} + m_{Se} = m_{mol}/N_{av}$ is the mass of a SMSC molecule. In the $Mn^{2+}$ case $L = 0$ and then $P = -\mu_e g \langle S \rangle$, and

$$M_m = (x/m) g \mu_B \langle S \rangle \ , \tag{3}$$

where we neglected opposite directions of $M_m$ and $S$. In $Fe^{2+}$ this problem requires a more careful study. The mean iron spin $\langle S \rangle$ can be calculated using isolated $Fe^{2+}$ ion wave functions for the $^5E$ term (see Sev. IV). It was found[10,14] that the mean spin of an Fe ion $\langle S \rangle$ is proportional to the magnetic moment $\langle M \rangle = \langle L + 2S \rangle$: $\langle S \rangle = k \langle M \rangle$, where $k = 0.447$ for $Zn_{1-x}Fe_xSe$ and $k = 0.444$ for $Cd_{1-x}Fe_xSe$, whereas for the spin-only case $k = \frac{1}{2}$. The smaller $k$ value (with respect to the spin-only case) reflects the contribution of the nonvanishing orbital momentum to the magnetization. We notice that this contribution is rather small ($\approx 10\%$) since it results from the admixture of the excited $^5T$ term.[5] The coefficient $k$ depends slightly on temperature as well as on the magnetic field but its variation is far below typical experimental accuracy of excitation splitting, and we therefore assume the constant $k$ value in further considerations.

A similar analysis performed for a Fe-Fe pair (see Sec. IV) shows that also in this case the pair's spin is proportional to the pair magnetic moment with the coefficient $k = 0.462$ ($Zn_{1-x}Fe_xSe$) and $k = 0.469$ ($Cd_{1-x}Fe_xSe$). The difference in $k$ for isolated ions and pairs is irrelevant [cf. Eq. (10) and the extended-nearest-neighbor pair approximation (ENNPA) in Sec. IV] and therefore one can assume that macroscopic magnetization measures $\langle S \rangle$ (at least for not very concentrated crystal, for which ENNPA would apply) and that the proportionality factor $k$ is practically the same as for a single ion. Under this assumption we get for the magnetization

$$M_m = \langle M \rangle (\mu_B x/m) = \langle S \rangle (\mu_B/k)(x/m) \ . \tag{4}$$

The full Hamiltonian describing conduction and valence bands of $Cd_{1-x}Fe_xSe$ can be obtained as a sum of the Hamiltonian (1) (with $j = \frac{1}{2}$ and $\frac{3}{2}$) and the well-known[17] Hamiltonian of wurtzite crystals. In the center of the Brillouin zone the total Hamiltonian matrix for the valence band reads[17,18]

$$\begin{pmatrix}
\delta\cos\theta & \delta\sin\theta & 0 & 0 & 0 & 0 \\
\delta\sin\theta & -2\Delta_2 - \delta\cos\theta & -\sqrt{2}\Delta_3 & 0 & 0 & 0 \\
0 & -\sqrt{2}\Delta_3 & -\Delta_1 - \Delta_2 + \delta\cos\theta & 0 & 0 & \delta\sin\theta \\
0 & 0 & 0 & -\delta\cos\theta & \delta\sin\theta & 0 \\
0 & 0 & 0 & \delta\sin\theta & -2\Delta_2 + \delta\cos\theta & \sqrt{2}\Delta_3 \\
0 & 0 & \delta\sin\theta & 0 & \sqrt{2}\Delta_3 & -\Delta_1 - \Delta_2 - \delta\cos\theta
\end{pmatrix} , \tag{5}$$

where $\delta = \frac{1}{2}(N_0\beta)\langle S \rangle$, $\beta = \langle X|J|X \rangle$ is an exchange integral for the valence band,[15] $\Delta_1$ is the crystal-field splitting constant due to the noncubic crystal field, and $\Delta_2$ and $\Delta_3$ are constants of the spin-orbit interaction. The matrix (5) is written in the standard basis function set: $X_{+\uparrow}, X_{+\downarrow}, Z_\uparrow, X_{-\uparrow}, X_{-\downarrow}, Z_\downarrow$, where $X_+ = (1/\sqrt{2})(X + iY)$, $X_- = (1/\sqrt{2})(X - iY)$, and $\uparrow, \downarrow$ denote the spin states. In the similar manner the conduction-band Hamiltonian matrix reads

$$\begin{pmatrix}
E_g + \tau\cos\theta & \tau\sin\theta \\
\tau\sin\theta & E_g - \tau\cos\theta
\end{pmatrix} , \tag{6}$$

where $E_g$ is the energy gap, $\tau = \frac{1}{2}x(N_0\alpha)\langle S \rangle$, and $\alpha = \langle S|J|S \rangle$ is the conduction-band exchange integral. The basis functions in this case are $S_\uparrow, S_\downarrow$.

On the basis of Hamiltonians (5) and (6) an energy-level diagram of $Cd_{1-x}Fe_xSe$ can be constructed, showing conduction band and valence bands $A$, $B$, and $C$ as a function of the Fe spin $\langle S \rangle$. This is shown as in Fig. 1 for $\theta = 0°$, 45°, and 90°. We note isotropic splitting of the conduction band: $E_c = E_g \pm \tau$. On the other hand anisotropy and mixing between valence- band states can be well observed. Only for $\theta = 0°$ there is no mixing of band $A$ ($X_{+\uparrow}, X_{-\downarrow}$) with the others and the splitting of band $A$ is proportional to $\delta$: $E_A = \pm\delta$. Therefore, optical transitions from the $A$ band to the conduction band for $B \| c$ can be used for determination of $N_0\alpha - N_0\beta$ in the similar way as for the cubic crystals:

$$\Delta E = E_d - E_a = (N_0\alpha - N_0\beta)x\langle S \rangle = (N_0\alpha - N_0\beta)mkM_m/\mu_B \ , \tag{7}$$

where $E_d, E_a$ are energies of optical transitions $a, d$ denoted in Fig. 1.

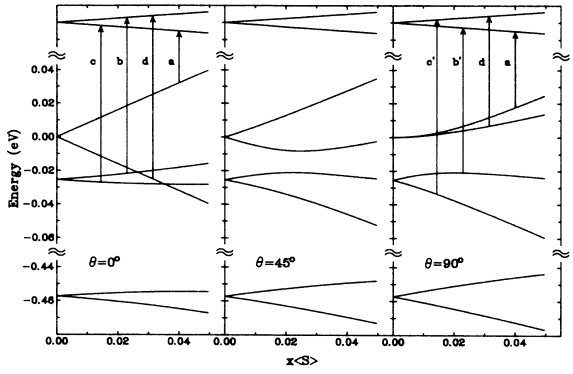


FIG. 1. Calculated diagram of energy levels of conduction and valence bands of $Cd_{1-x}Fe_xSe$ as a function of mean spin $x\langle S\rangle$ for different angles between the magnetic field and the crystal hexagonal axis: (a) $\theta=0°$, (b) $\theta=45°$, and (c) $\theta=90°$. The following parameters were used: $\Delta_1=0.069$ eV, $\Delta_2=0.138$ eV, $\Delta_3=0.151$ eV (Ref. 39), $N_0\alpha=0.25$ eV, and $N_0\beta=-1.6$ eV. The arrows indicate observed optical transitions.

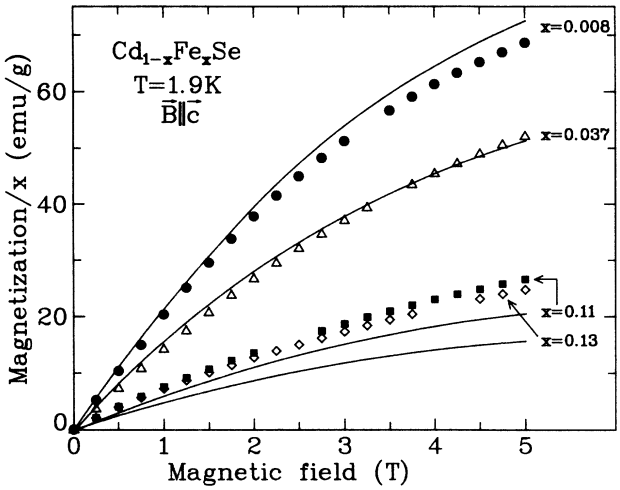


FIG. 2. Magnetization of $Cd_{1-x}Fe_xSe$ per one Fe ion at $T=1.9$ K for **B** parallel to the **c** axis ($\theta=0°$). The solid lines show calculated magnetization as described in Sec. IV.

## III. EXPERIMENT

The $Cd_{1-x}Fe_xSe$ crystals for testing ($x\leq 0.13$) were grown by the modified Bridgman technique at the Institute of Physics, Polish Academy of Sciences. The actual iron concentration was determined from the free exciton energy according to the formula[19]

$$E_{ex}(x)=(14725+9564x+7964x^2) \quad (8)$$

in $cm^{-1}$. This method also provided a useful way of checking the homogeneity of our crystals. We found that the variation of $x$ along the sample could amount from $\Delta x=0.001$ to 0.005 (for the highest $x$).

We measured free exciton magnetoreflectance in the Faraday configuration (light wave vector along magnetic field) for circularly polarized light ($\sigma^+$,$\sigma^-$ polarizations) at $T=1.9$ K and the magnetic field $B\leq 5$ T. The magnetic field was oriented parallel and perpendicular to the crystal hexagonal $c$ axis. Reflectance was measured on cleaved surfaces; neither mechanical polishing nor chemical etching was performed.

Magnetization was measured by means of a superconducting quantum interference device magnetometer on the very same samples on which magnetoreflectance was measured. The temperature of the samples during experiment was the same as that during optical work ($T=1.9$ K), as well as the magnetic field range ($B\leq 5$ T). We mention that the previous investigation of $Cd_{1-x}Fe_xSe$ crystals used by us suggested existence of some paramagnetic impurities, other than $Fe^{2+}$.[14] The concentration of these impurities was estimated for at about 1% of the actual $Fe^{2+}$ content.[14]

## IV. MAGNETIZATION

In Fig. 2 we show magnetization $M_m$ (per unit mass) of $Cd_{1-x}Fe_xSe$, $x=0.008$, 0.037, 0.11, and 0.13 at $T=1.9$ K as a function of magnetic field, for $B$ parallel to the $c$ axis. The data presented above reveal typical features observed previously for $Zn_{1-x}Fe_xSe$,[20] $Cd_{1-x}Fe_xTe$,[21] and $Cd_{1-x}Fe_xSe$.[11]

Magnetization varies strongly with applied magnetic field. No saturation effects of $M_m$ are observed, including crystals with very low Fe concentration, in contrast with the behavior of Mn-type SMSC's.

Magnetization per one Fe ion ($M_m/x$) decreases with increasing $x$ indicating antiferromagnetic interaction between Fe ions.

Due to the crystal hexagonal structure magnetization is strongly anisotropic, which is exemplified in Fig. 3 for $Cd_{1-x}Fe_xSe$: $x=0.008$ in the field parallel and perpendicular to the crystal $c$ axis.

We describe our magnetization data using the "crystal-field" model developed for Fe-based SMSC's,[22,23] in particular, for hexagonal materials.[24] In this model

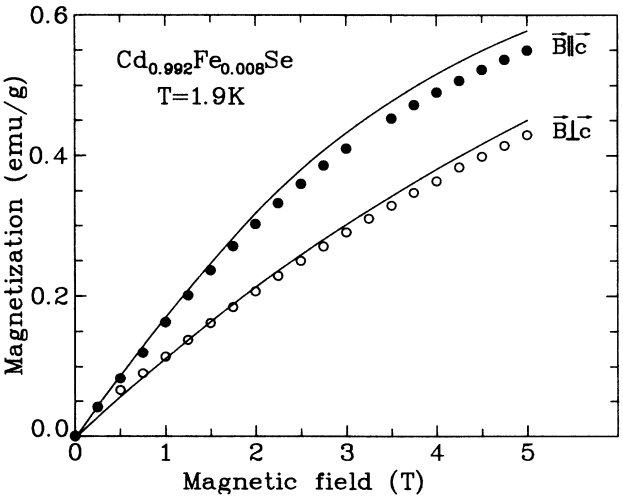


FIG. 3. Magnetization of $Cd_{0.992}Fe_{0.008}Se$ at $T=1.9$ K for **B** parallel ($\theta=0°$) and perpendicular ($\theta=90°$) to the crystal **c** axis. The solid lines show calculated magenetization as described in Sec. IV.

one assumes that the Fe ion system can be factorized into Fe-Fe pairs coupled by principally long-range interaction [so-called ENNPA (Ref. 25)]. Therefore magnetization (or many other properties) per one ion can be expressed in the following way:

$$M=\sum_{i}^{\infty} M_i(J_i)P_i(x)/2 \ , \tag{9}$$

where $M_i$ $(J_i)$ is the pair magnetization depending on the Fe-Fe $d$-$d$ exchange integral $J_i$ and $P_i(x)$ is the probability of finding at least one Fe ion in the $i$th coordination sphere (for details we refer to Ref. 25). We note that ENNPA is limited to rather small concentrations of magnetic ions ($x<0.05$). It was found during calculations (for both cubic and hexagonal structures) that the long-range interaction is not so relevant for Fe-based SMSC's as it was for Mn-type SMSC and therefore Eq. (9) can be reduced to the sum of isolated (i.e., noninteracting) ions and nearest-neighbor pairs:

$$M=M_m P_m(x)+M_p P_p(x)/2 \ , \tag{10}$$

where $M_s$ and $M_p$ are magnetizations of an isolated ion and the Fe-Fe pair, respectively. Assuming random distribution of the Fe ion in the crystal we have $P_s(x)=(1-x)^{12}$ and $P_p(x)=12x(1-x)^{18}$. Magnetization $M_s$ and $M_p$ can be evaluated from the magnetic moments

$$\begin{aligned} M_s&=\mu_B\left[\sum_i \langle\phi_i|\mathbf{L}+2\mathbf{S}|\phi_i\rangle\exp(-E_i/kT)\right]\Big/\left[\sum_i \exp(-E_i/kT)\right] , \\ M_p&=\mu_B\left[\sum_i \langle\Phi_i|(\mathbf{L}_1+2\mathbf{S}_1)+(\mathbf{L}_2+2\mathbf{S}_2)|\Phi_i\rangle\exp(-E_i/kT)\right]\Big/\left[\sum_i \exp(-E_i/kT)\right] . \end{aligned} \tag{11}$$

The energies $E_i$ and eigenvalues $\phi,\Phi$ result from the numerical diagonalization of isolated ion or pair Hamiltonians, respectively. In this paper we used basically the same Hamiltonian as in Ref. 24, however, expressing hexagonal distortion in a way more common in the literature:[26]

$$H_{\rm cf}=-\tfrac{2}{3}B_4(O_4^0+20\sqrt{2}O_4^3)+B_2^0O_2^0+B_4^0O_4^0 \ . \tag{12}$$

The matrix of Hamiltonian (12) contains only five different elements; diagonal elements $-6Dq$, $4Dq+2/3v$, and $4Dq-1/3v$; the off diagonal elements $v'$ and $-v'$.

The full Hamiltonian for an isolated $Fe^{2+}$ ion can now be written as

$$H=H_{\rm cf}+H_{\rm s.o.}+H_B \ , \tag{13}$$

where $H_{\rm s.o.}=\lambda\mathbf{S}\cdot\mathbf{L}$, is the spin-orbit interaction, $H_B=\mu_B(\mathbf{L}+2\mathbf{S})\cdot\mathbf{B}$ is the Zeeman term, and the $z$ axis was chosen along the [111] direction (i.e., parallel to the crystal $c$ axis). The presence of trigonal distortion in the Hamiltonian (12) causes splitting of triplets $T_1,T_2$ into singlets and doublets ($T_1-A_2,E$ and $T_2-A_1,E$).[6] Since the Hamiltonian matrix is parametrized by material constants $Dq$, $v$, $v'$ and $\lambda$, the obtained energies can be used for the estimation of these parameters for $Cd_{1-x}Fe_xSe$. We used for that very recently measured energies of optical transition $A_1\rightarrow A_2$ [13 $cm^{-1}$ (Ref. 19)]. $A_1\rightarrow E$ [17.6 $cm^{-1}$ (Ref. 19)] as well as zero-phonon-line energy for $^5E\rightarrow{}^5T$ transition [2375 $cm^{-1}$ (Ref. 27)]. The best fit was found for $Dq=257$ $cm^{-1}$, $\lambda=-93.8$ $cm^{-1}$, $v=31$ $cm^{-1}$ and $v'=38$ $cm^{-1}$. For a Fe-Fe pair the Hamiltonian is assumed in the form[22,24]

$$H=H_1+H_2-2J_{dd}\mathbf{S}_1\mathbf{S}_2 \ , \tag{14}$$

where $H_1,H_2$ are isolated ion Hamiltonians (13) and the $d$-$d$ exchange interaction between these ions is described by the isotropic Heisenberg-type exchange. $J_{dd}$ denotes the $d$-$d$ nearest-neighbor exchange integral. This parameter was estimated for $Cd_{1-x}Fe_xSe$ from the high-temperature susceptibility giving $J_{dd}=-19$ K.[28,3]

Numerical solutions of Hamiltonians (13) and (14) are used for calculations of magnetic moments in Eq. (11) (and the coefficient as discussed in Sec. II). In Fig. 4 we display magnetic moments of an isolated Fe ion as well as the Fe-Fe pair for $B$ parallel to the hexagonal axis. We note that in the considered field range the magnetic moment of the Fe-Fe pair is much smaller than the isolated ion moment, roughly by 2 orders of magnitude. Finally

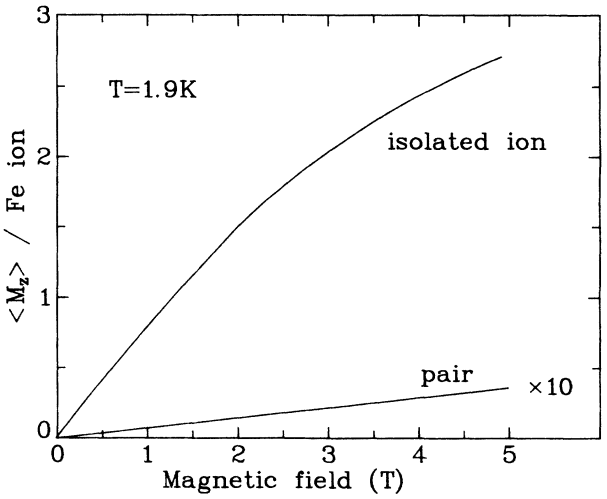


FIG. 4. Calculated magnetic moment of an isolated Fe ion and Fe-Fe pair shown per one Fe ion for $Dq=257$ $cm^{-1}$, $\lambda=-93.8$ $cm^{-1}$, $v=31$ $cm^{-1}$, $v'=38$ $cm^{-1}$, and $J=-19$ K (note multiplication factor for the Fe-Fe pair).

macroscopic magnetization per unit mass should read

$$M_m(x)=[M_m P_m(x)+M_p P_p(x)/2]x/m \ . \quad (15)$$

We note that this formula is restricted to rather low Fe concentrations.

In view of the small Fe-Fe pair contributions to Eq. (15) (for not very high fields), in practice one can describe magnetization taking into account only isolated ion contribution. This simplification is accurate to 1% for $x<0.1$. This result justifies *ex post* assumption done in Ref. 20. The phenomenological parameter $A$, introduced in Ref. 20 corresponds to probability $P_s(x)$. For higher $x$ ($x=0.11$ and 0.13) $A>P_s(x)$,[20] which clearly indicates that for these concentrations there is significant contribution to the real magnetization from clusters larger than singles and pairs.

In Figs. 2 and 3 we show results of magnetization calculations for our crystals. We find satisfactory matching with the experimental data for the crystals with low Fe content ($x\leq 0.04$), although no fitting procedure was applied. Moreover magnetization anisotropy is well reproduced (Fig. 3). Small departure from the experimental data for $Cd_{0.992}Fe_{0.008}Se$ (Figs. 2 and 3) are completely within accuracy of Fe concentration of this sample ($x=0.008\pm0.001$). On the other hand the deviations observed for the highest concentrations ($x=0.11$, 0.13) cannot be accounted for the variation or inhomogeneity of $x$ ($\Delta x\approx 0.005$) but they result from the fact that the approximation of the Fe ion system only by single ions and pairs is invalid for $x>0.05$, as we have noted above. Deviations between experimental data and theory for $x=0.11$ and 0.13 clearly demonstrate the important role of Fe clusters larger than pairs. In order to estimate the contribution of these clusters we assumed that the difference between experimental data and theory given by (15) results from larger clusters, whose magnetic moment $M_c$ (per one ion in the cluster) is concentration independent:

$$M_m(x)=\{M_s P_s(x)+M_p P_p(x)/2+M_c[1-P_s(x)-P_p(x)]\}x/m \ . \quad (16)$$

Using this crude assumption we estimated $M_c\approx 0.13M_s$ for $x=0.11$ and $M_c\approx 0.16M_s$ for $x=0.13$. Assuming that $M_c$ is roughly the same also for lower $x$ one has an additional correction to the magnetization calculated with the help of Eq. (25). This correction amounts to $\approx 3\%$ of the total $M_m$ value for $x=0.04$ and $\approx 5.5\%$ for $x=0.05$. Calculations for clusters larger than pairs were not performed because of large dimensions of corresponding Hamiltonian matrices to be diagonalized ($1000\times 1000$ for a three-ion cluster).

## V. MAGNETOREFLECTANCE

Typical $A$ and $B$ exciton magnetoreflectance spectra are demonstrated in Fig. 5 ($x=0.038$,**B**$\|$**c**) and Fig. 6 ($x=0.044$,**B**$\perp$**c**). A variation of exciton energy levels with the magnetic field is exemplified in Fig. 7 ($x=0.008$, *a*, **B**$\|$**c**; *b*, **B**$\perp$**c**) and Fig. 8 ($x=0.037$; *a*, **B**$\|$**c**; *b*, **B**$\perp$**c**). The overall exciton splitting is in accordance with the predictions presented in Sec. II: for $B$ parallel to the **c** axis exciton $A$ is strongly split, whereas exciton $B$ is split very weakly ($E_c-E_b$ splitting is actually smaller than the experimental accuracy). For **B** perpendicular to the **c** axis the situation is somehow reversed. Such behavior was also observed for $Cd_{1-x}Mn_xSe$.[18,29] The exciton lines *a*, *b*, *c*, and *d* correspond to the interband transitions from Fig. 1.

We also notice the relaxation of selection rules for **B**$\perp$**c** (Figs. 5–8) resulting from valence-band states mixing for **B**$\perp$**c**.

In Fig. 9 we show exciton splitting ($E_d-E_a$,**B**$\|$**c**) for several samples. A similar variation of the splitting with

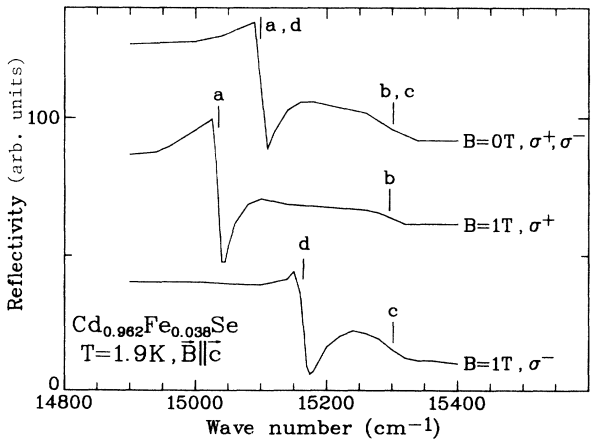


FIG. 5. Exciton reflectance spectra for $Cd_{0.962}Fe_{0.038}Se$ at $T=1.9$ K for **B**$\|$**c**.

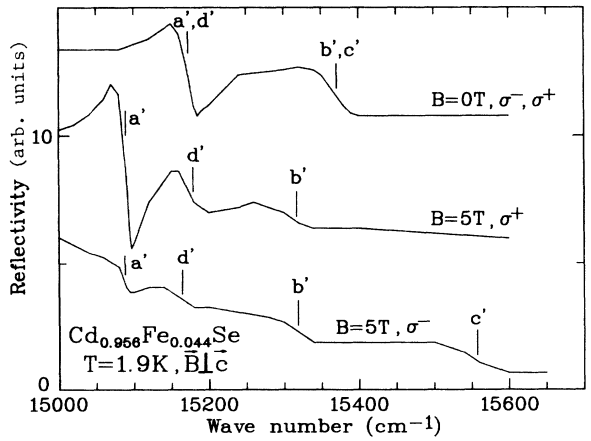


FIG. 6. Exciton reflectance spectra for $Cd_{0.956}Fe_{0.044}Se$ at $T=1.9$ K for **B**$\perp$**c**.

magnetic field is observed as for magnetization (Fig. 2).

We found that the exciton splitting $E_d - E_a$ is proportional to the magnetization for each sample. In Fig. 10 we plotted $E_d - E_m$ versus $mkM_m/\mu_B$, as suggested by Eq. (7). A common straight line is obtained for all samples. This strongly suggests that indeed exciton (and band) splittings are parametrized by macroscopic magnetization and, therefore, by mean spins [cf. Eq. (4)]. From the slope of the line in Fig. 10 we determine $N_0\alpha - N_0\beta = (1.85 \pm 0.10)$ eV, a smaller value than

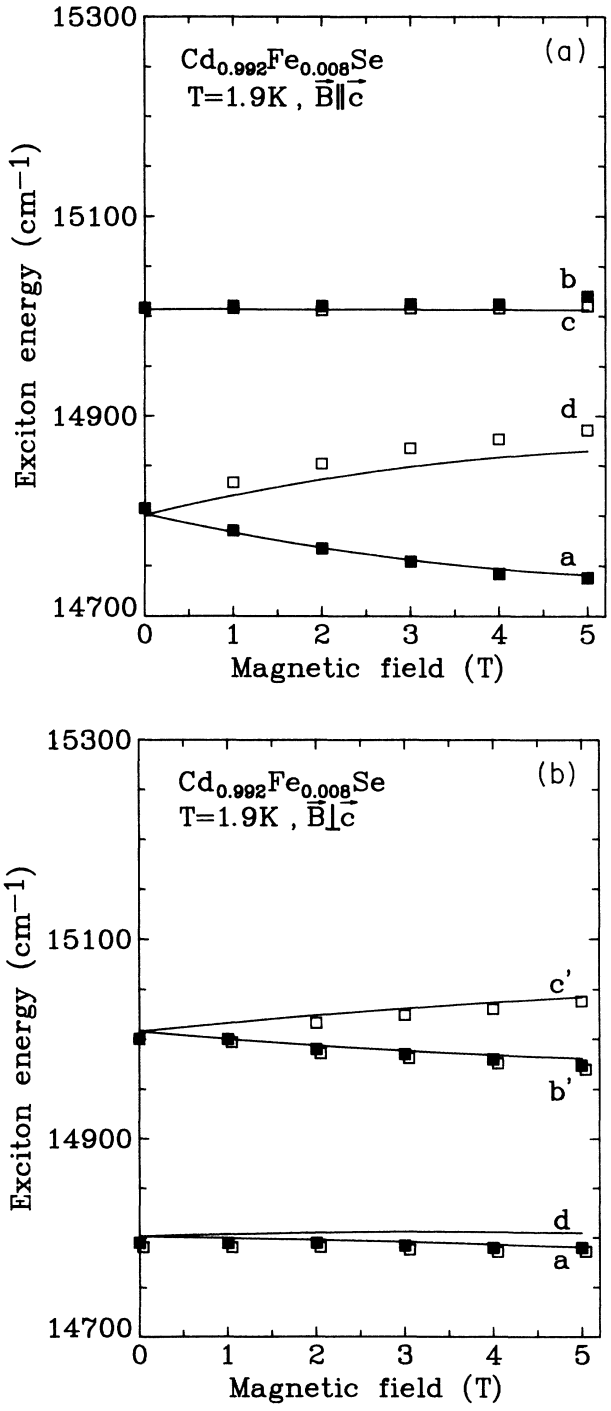


FIG. 7. Energies of the exciton lines ($a, b - \sigma^+$; $c, d - \sigma^-$) in $Cd_{0.992}Fe_{0.008}Se$ at $T = 1.9$ K for **B** (a) parallel and (b) perpendicular to the crystal hexagonal axis. The lines show results of theoretical calculations with $N_0\alpha = 0.25$ eV and $N_0\beta = -1.6$ eV and experimental magnetization (shown in Fig. 3).

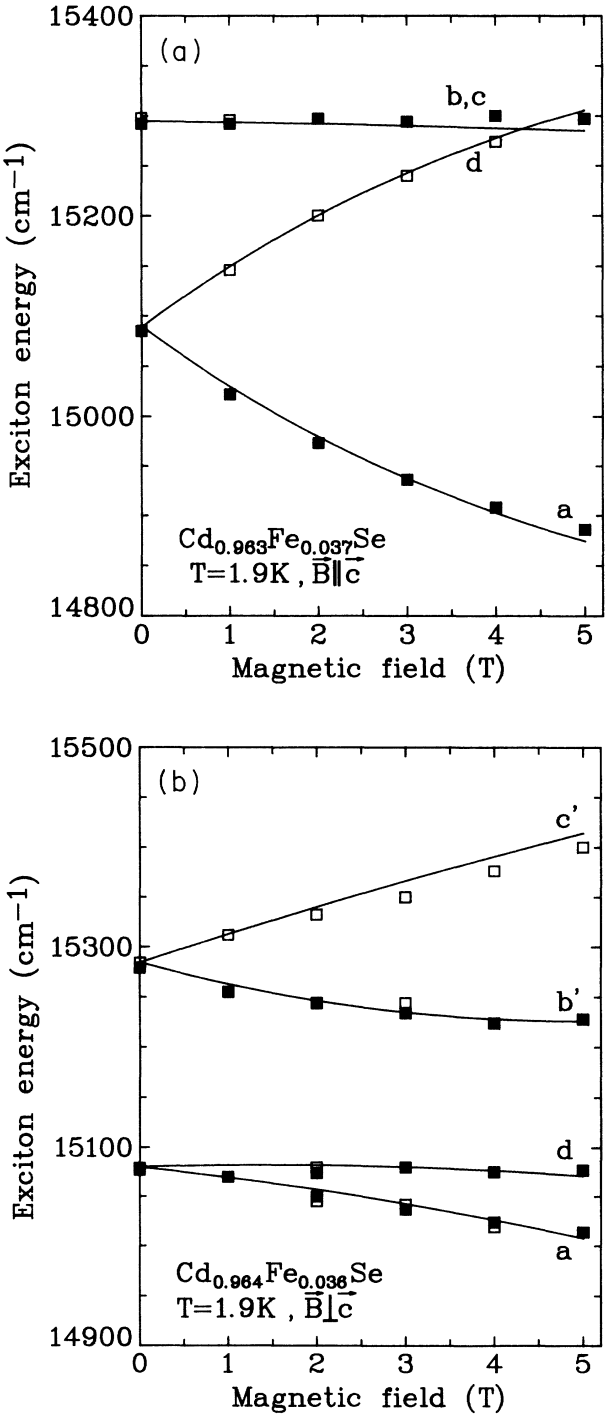


FIG. 8. Energies of the exciton lines ($a, b - \sigma^+$; $c, d$-$\sigma^-$) in $Cd_{0.963}Fe_{0.037}Se$ at $T = 1.9$ K for **B** (a) parallel and (b) perpendicular to the crystal hexagonal axis. The lines show results of theoretical calculations with $N_0\alpha = 0.25$ eV and $N_0\beta = -1.6$ eV and parametrized by (a) experimental and (b) calculated magnetization.

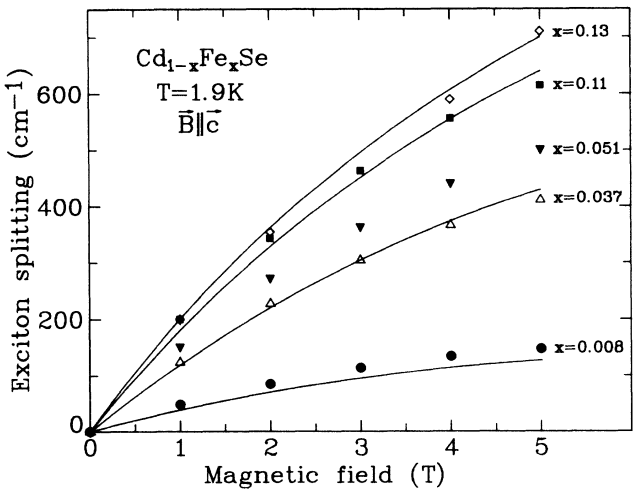


FIG. 9. Exciton splitting ($E_d$-$E_a$) in $Cd_{1-x}Fe_xSe$ for various $x$ at $T=1.9$ K for **B** parallel to hexagonal **c** axis. The lines show calculated exciton splitting [Eq. (7)] with $N_0\alpha=0.25$ eV and $N_0\beta=-1.6$ eV parametrized by experimental magnetization (except of $x=0.051$, whose magnetization data were not available).

(2.13±0.15) eV, previously reported by us.[14] However the previous value was estimated based on low-field susceptibility.[14] The present way of evaluation of exchange integrals is much more reliable.

We should comment here on the paramagnetic impurities present in our crystals (Sec. III). In principle both exciton splitting and magnetization should be corrected for these impurities,[14] however, in the case of relatively strong magnetic field ($B>1$ T) these corrections are not so important as they were for low fields ($B<0.1$ T). In fact they are smaller than experimental errors and therefore they were not taken into account.

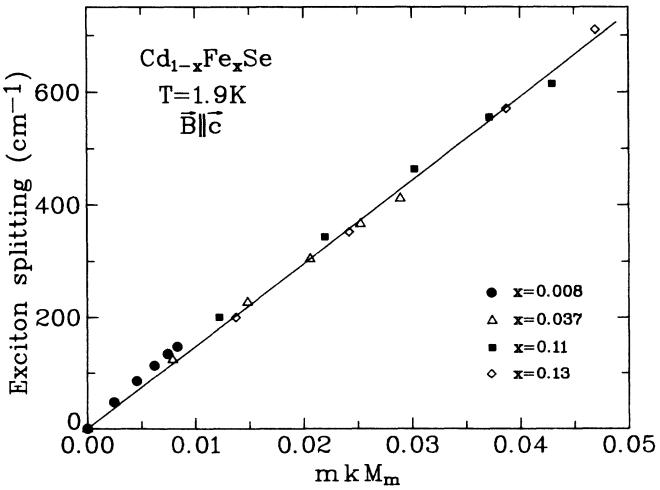


FIG. 10. Exciton splitting ($E_d-E_a$) of $Cd_{1-x}Fe_xSe$ vs magnetization expressed in $mkM_m$. $T=1.9$ K and **B** is parallel to the hexagonal $c$ axis. The strainght line shows theoretical dependence for $N_0\alpha-N_0\beta=-1.85$ eV.

The individual $N_0\alpha$ and $N_0\beta$ values can, in principle, be evaluated with the help of the exciton lines $b$ and $c$. It follows from Eqs. (5) and (6) that for **B**||**c**

$$E_c-E_b\approx-(N_0\alpha+\Omega N_0\beta)x\langle S_z\rangle\ , \tag{17}$$

where $\Omega=\dfrac{\Delta_1-\Delta_2}{(\Delta_1-\Delta_2)^2+8\Delta_3^2}$ .

Combining (17) with (7) one obtains

$$1=\frac{E_c-E_b}{E_d-E_a}=\frac{1+\Omega\beta/\alpha}{\beta/\alpha-1}$$

and then

$$\beta/\alpha=(l+1)/(1-\Omega)\ . \tag{18}$$

Since the splitting of exciton lines $b$ and $c$ is very small, $|E_c-E_b|=(10\pm15)$ cm$^{-1}$, we have a rather uncertain $\beta/\alpha$ value $-10<\beta/\alpha<-3$ and finally $0.17<N_0\alpha<0.46$ eV, $-1.4>N_0\beta>-1.7$ eV. However $N_0\alpha$ was determined independently from the Raman spin-flip experiment,[11] giving $N_0\alpha=(0.225\pm0.005)$ eV, the value not corrected by the $k$ factor (Sec. II). Performing this correction we get

$$N_0\alpha=(+0.25\pm0.01)\text{ eV}$$

and then

$$N_0\beta=(-1.6\pm0.1)\text{ eV}\ .$$

Having determined exchange constants one is able to calculate the band structure precisely from (5) and (6) using experimental magnetization as a parameter. Results of such calculations are shown in Figs. 7, 8, and 9 (we stress that no further fitting procedure was performed). We find a reasonable description of the experimental data for both parallel and perpendicular configurations, which proves that, in fact, band splittings are parametrized by macroscopic magnetization, as predicted in Sec. II. Detailed analysis of the data reveals similar problems with actual Fe concentration as was already mentioned for magnetization. In particular the $Cd_{0.992}Fe_{0.0008}Se$ sample reveals different local $x$ for **B**||**c** and **B**⊥**c** measurements ($x=0.009$ and $x=0.007$, respectively). Although calculations which take into account exact local concentration instead of mean $x$ value ($x=0.008$) would provide a better matching with experimental data, we refrained from doing that since in this case magnetization also would have to be scaled. We believe that at the present stage the conclusion about parametrization of band splitting by macroscopic magnetization is more straightforward in spite of some discrepancy between experiment and theory. We must note, however, that major uncertainty in comparing experimental data and calculations is due to the inhomogeneity of our crystals.

Finally let us comment on chemical trends of exchange constants in SMSC's. The conduction-band exchange integral in $Cd_{1-x}Fe_xSe$ is practically the same as for $Zn_{1-x}Fe_xSe$ and $Cd_{1-x}Mn_xSe$ (Table I). The present

TABLE I. Exchange constants in semimagnetic semiconductors.

| Material | $N_0\alpha$ (eV) | $N_0\beta$ (eV) | $J_{NN}/k_B$ (K) |
|---|---|---|---|
| $Zn_{1-x}Fe_xSe$ | 0.22 (Ref. 10) | −1.74 (Ref. 10) | −22 (Ref. 28) |
| $Cd_{1-x}Fe_xSe$ | 0.25 (Ref. 11) | −1.9 (Ref. 14) | −19 (Ref. 3) |
| | | −1.6 (this paper) | |
| | | −1.45 (Ref. 40) | |
| | 0.258 (Ref. 41) | −1.53 (Ref. 41) | |
| $Hg_{1-x}Fe_xSe$ | | | −18 (Ref. 3) |
| $Zn_{1-x}Mn_xSe$ | 0.26 (Ref. 32) | −1.31 (Ref. 32) | −12.6 (Ref. 33) |
| $Cd_{1-x}Mn_xSe$ | 0.23 (Ref. 29) | −1.26 (Ref. 29) | −7.9 (Ref. 35) |
| | 0.26 (Ref. 34) | −1.11 (Ref. 18) | −8.3 (Ref. 36) |
| | | | −10.6 (Ref. 37) |
| $Hg_{1-x}Mn_xSe$ | | | −11 (Ref. 37) |
| | | | −6 (Ref. 38) |

value of the valence-band integral $N_0\beta$ is very close to the value of $Zn_{1-x}Fe_xSe$ and substantially larger than for $Cd_{1-x}Mn_xSe$. In general, one finds a similar situation for both Mn and Fe SMSC's families: $s,p$-$d$ exchange integrals are comparable for Zn and Cd selenides within each family (Table I). The higher values of the valence-band integrals for Fe SMSC's should be correlated with the $d$-$d$ exchange integrals. It is suggested for Fe-based SMSC's that superexchange is the dominant mechanism of the $d$-$d$ interaction,[3] similarly as for Mn-type materials.[1,30,31] In this case the coupling between Fe $d$ electrons occurs via valence-band states (electrons) and therefore the probability of electron hoping (transfer) between $d$ states and valence-band states (described by $N_0\beta$) should be directly related to the $d$-$d$ exchange integral $J_{dd}$. In particular $N_0\beta \sim V^2$ and $J_{dd} \sim V^4$, where $V$ is the matrix element describing hybridization, i.e., electron hoping between the valence-band and Fe $d$ level (cf. Refs. 30 and 31). We find that $N_0\beta$ is larger for $Cd_{1-x}Fe_xSe$ by a factor $\frac{1.6}{1.1}=1.45$ in respect to $Cd_{1-x}Mn_xSe$ ($\frac{1.74}{1.31}=1.33$ for ZnSe). Assuming that this increase of $N_0\beta$ results mainly from a stronger hybridization, one can expect a larger $J_{dd}$ parameter by a factor $(1.45)^2=2.1$ (1.8 for ZnSe), which compares favorably with the experimental $J_{dd}$ value: $J_{dd}(Cd_{1-x}Fe_xSe)=-19$ K $\approx 2.1 J_{dd}(Cd_{1-x}Mn_xSe)=-18$ K, $J_{dd}(Zn_{1-x}Fe_xSe)=-22$ K $\approx 1.8 J_{dd}(Zn_{1-x}Mn_xSe)=-23$ K. Detailed analysis of the chemical trends in $d$-$d$ and $p$-$d$ exchange interactions in these materials require however further study, in particular, the location of the Fe $d$ level relative to the valence band is of great importance.[31]

## VI. CONCLUSIONS

We demonstrated for hexagonal $Cd_{1-x}Fe_xSe$ that the band splittings are parametrized by macroscopic magnetization, similarly as for $Zn_{1-x}Fe_xSe$. Combining free-exciton splitting data with the magnetization results obtained on the same samples we determined exchange integral for the valence band. We discussed chemical trends of $s,p$-$d$ and $d$-$d$ exchange interaction for Fe- and Mn-type SMSC's.

We also presented a theoretical model for low Fe concentration magnetization, which seems to provide a reasonable description of the experimental data. In particular, magnetization anisotropy resulting from the crystal hexagonal structure is well recovered. Moreover we found that at not very high magnetic fields ($B \leq 5T$), and $x < 0.05$, the major contribution to the magnetization results from the noninteracting Fe ions, which is an advantage from the practical point of view: magnetization calculations can be thus considerably simplified.

## ACKNOWLEDGMENTS

The crystals for testing were kindly supplied by Professor A. Mycielski. We also thank Professor J. A. Gaj and Professor M. Grynberg for helpful discussions.

[1] See, *Semiconductors and Semimetals*, Vol. 25 of *Diluted Magnetic Semiconductors*, edited by J. K. Furdyna and J. Kossut (Academic, New York, 1988), and review paper, J. K. Furdyna, J. Appl. Phys. **64**, R29 (1988).

[2] A. Mycielski, J. Appl. Phys. **63**, 3279 (1988).

[3] A. Twardowski, J. Appl. Phys **67**, 5108 (1990).

[4] W. Low and M. Weger, Phys. Rev. **118**, 1119 (1960).

[5] G. A. Slack, S. Roberts, and J. T. Vallin, Phys. Rev. **187**, 511 (1969).

[6] J. Mahoney, C. Lin, W. Brumage, and F. Dorman, J. Chem. Phys. **53**, 4286 (1970).

[7] J. T. Vallin, G. A. Slack, and C. C. Bradley, Phys. Rev. B **2**, 4406 (1970).

[8] J. T. Vallin, Phys. Rev. B **2**, 2390 (1970).

[9] J. M. Baranowski, J. W. Allen, and G. L. Pearson, Phys. Rev. **160**, 627 (1967).

[10] A. Twardowski, P. Glod, W. J. M. de Jonge, and M. Demianiuk, Solid State Commun. **64**, 63 (1987).

[11] D. Heiman, A. Petrou, S. H. Bloom, Y. Shapira, E. D. Isaacs, and W. Giriat, Phys. Rev. Lett. **60**, 1876 (1988); D. Heiman, E. D. Isaacs, P. Becla, A. Petrou, K. Smith, J. Marsella, K. Dwight, and A. Wold, in *Proceedings of 19th International Conference on the Physics of Semiconductors, Warsaw, 1988*, edited by W. Zawadzki (Institute of Physics, Polish Academy

of Sciences, Wroclaw, 1989), p. 1539.
[12]A. Petrou, X. Liu, G. Waytena, J. Warnock, and W. Giriat, Solid State Commun. **61**, 767 (1987).
[13]X. Liu, A. Petrou, J. Warnock, B. T. Jonker, G. A. Prinz, and J. J. Krebs, Phys. Rev. Lett. **63**, 2280 (1990).
[14]A. Twardowski, K. Pakula, M. Arciszewska, and A. Mycielski, Solid State Commun. **73**, 601 (1990).
[15]J. A. Gaj, J. Ginter, and R. R. Galazka, Phys. Status Solidi B **89**, 655 (1978).
[16]S. H. Liu, Phys. Rev. **121**, 451 (1960).
[17]G. L. Bir and G. E. Pikus, *Symmetry and Strain-Induced Effects in Semiconductors* (Wiley, New York, 1974).
[18]R. L. Aggarwal, S. N. Jasperson, J. Stankiewicz, Y. Shapira, S. Foner, B. Khazai, and A. Wold, Phys. Rev. B **28**, 6907 (1983).
[19]D. Scalbert, J. Cernogora, A. Mauger, C. Benoit à la Guillaume, and A. Mycielski, Solid State Commun. **69**, 453 (1989); J. A. Gaj (private communication).
[20]A. Twardowski, M. von Ortenberg, and M. Demianiuk, J. Cryst. Growth **72**, 401 (1985).
[21]C. Testelin, A. Mauger, C. Rigaux, M. Guillot, and A. Mycielski, Solid State Commun. **71**, 923 (1989).
[22]A. Twardowski, H. J. M. Swagten, T. F. H. v. d. Wetering, and W. J. M. de Jonge, Solid State Commun. **65**, 235 (1988).
[23]H. J. M. Swagten, A. Twardowski, W. J. M. de Jonge, and M. Demianiuk, Phys. Rev. B **39**, 2568 (1989).
[24]A. Twardowski, Solid State Commun. **68**, 1069 (1988).
[25]C. J. M. Denissen, H. Nishihara, J. C. van Gool, and W. J. M. de Jonge, Phys. Rev. B **33**, 7637 (1986); C. J. M. Denissen and W. J. M. de Jonge, Solid State Commun. **59**, 503 (1986); A. Twardowski, H. J. M. Swagten, W. J. M. de Jonge, and M. Demianiuk, Phys. Rev. B **36**, 7013 (1987).
[26]A. Abragam and B. Bleaney, *EPR of Transition Metal Ions* (Clarendon, Oxford, 1970), p. 372.
[27]M. Arciszewska (private communication).
[28]A. Twardowski, A Lewicki, M. Arciszewska, W. J. M. de Jonge, H. J. M. Swagten, and M. Demianiuk, Phys. Rev. B **38**, 10 749 (1988).
[29]M. Arciszewska and M. Nawrocki, J. Phys. Chem. Solids **47**, 309 (1986).
[30]B. E. Larson, K. C. Hass, H. Ehrenreich, and A. E. Carlsson, Solid State Commun. **56**, 347 (1985); Phys. Rev. B **37**, 4137 (1988).
[31]H. Ehrenreich, K. C. Hass, B. E. Larson, and N. F. Johnson, in *Diluted Magnetic (Semimagnetic) Semiconductors,* Vol. 89 of *Materials Research Society Proceedings Symposium, Boston, 1986,* edited by S. Von Molnar, R. L. Aggarwal, and J. K. Furdyna (MRS, Pittsburg, MA, 1987), p. 187.
[32]A. Twardowski, T. Dietl, and M. Demianiuk, Solid State Commun. **48**, 945 (1983); A. Twardowski, M. von Ortenberg, M. Demianiuk, and R. Pauthenet, Solid State State Commun. **51**, 849 (1984).
[33]T. M. Giebultowicz, J. J. Rhyne, and J. K. Furdyna, J. Appl. Phys. **61**, 3537 (1987); **61**, 3540 (1987).
[34]Y. Shapira, D. Heiman, and S. Foner, Solid State Commun. **44**, 1243 (1982).
[35]B. E. Larson, K. C. Hass, and R. L. Aggarwal, Phys. Rev. B **33**, 1789 (1986).
[36]Y. Shapira, S. Foner, D. H. Ridgley, K. Dwight, and A. Wold, Phys. Rev. B **30**, 4021 (1984).
[37]J. Spalek, A. Lewicki, Z. Tarnawski, J. K. Furdyna, R. R. Galazka, and Z. Obuszko, Phys. Rev. B **33**, 3407 (1986).
[38]R. R. Galazke, W. Dobrowolski, J. P. Lascaray, M. Nawrocki, A. Bruno, J. M. Broto, and J. C. Ousset, J. Magn. Magn. Mater. **72**, 174 (1988).
[39]D. W. Langer, R. N. Euwema, K. Era, and T. Koda, Phys. Rev. B **2**, 4005 (1970).
[40]O. W. Shih, R. L. Aggarwal, Y. Shapira, S. H. Bloom, V. Bindilatti, R. Kershaw, K. Dwight, and A. Wold, Solid State Commun. **74**, 455 (1990).
[41]D. Scalbert, M. Guillot, A. Mauger, J. A. Gaj, J. Cernogora, C. Benoit. à la Guillaume, and A. Mycielski (unpublished).